

An analysis of EEG networks and their correlation with cognitive impairment in preschool children with epilepsy

Eli Kinney-Lang^{a,b,*}, Michael Yoong^b, Matthew Hunter^b, Krishnaraya Kamath Tallur^c, Jay Shetty^c, Ailsa McLellan^c, Richard FM Chin^{†b,c}, Javier Escudero^{†a,b}

^a*School of Engineering, Institute for Digital Communications, The University of Edinburgh, Edinburgh EH9 3FB, United Kingdom*

^b*The Muir Maxwell Epilepsy Centre, The University of Edinburgh, Edinburgh EH8 9XD, United Kingdom*

^c*Royal Hospital for Sick Children, Edinburgh EH9 1LF, United Kingdom*

Abstract

Objective: Epilepsy in children is often accompanied by cognitive impairment (CI), causing significant quality of life effects for child and family. Early identification of subjects likely to develop CI could help inform strategies for clinicians. This paper proposes identifying characteristics correlated to CI in preschool children based on electroencephalogram (EEG) network analysis.

Methods: A multi-part processing chain analyzed networks from routinely acquired EEG of $n = 51$ children with early-onset epilepsy (0-5 y.o). Combinations of connectivity metrics (e.g. phase-slope index (PSI)) with network filtering techniques (e.g. cluster-span threshold (CST)) identified significant correlations between network properties and intelligence z -scores (Kendall's τ , $p < 0.05$). Predictive properties were investigated via 5-fold cross-validated classification for normal, mild/moderate and severe impairment classes.

Results: Phase-dependant connectivity metrics demonstrated higher sensitivity to measures associated with CI, while wider frequencies were present in CST filtering. Classification using CST was approximately 70.5% accurate, improving random classification by 55% and reducing classification penalties by half compared to naive classification.

Conclusions: Cognitive impairment in epileptic preschool children can be revealed and predicted by EEG network analysis.

Significance: This study outlines identifying markers for predicting CI in preschool children based on EEG network properties, and illustrates its potential for clinical application.

Keywords: Network analysis, signal processing, EEG graph networks, paediatric epilepsy, developmental impairment

*Corresponding author

† Authors contributed equally to the work.

Email address: e.kinney-lang@ed.ac.uk (Eli Kinney-Lang)

Highlights

- EEG network analysis correlates with cognitive impairment in preschool children with epilepsy.
- Network sensitivity to impairment improves with dense networks and phase-based connectivity measures.
- Classification reveals network features' predictive potential for clinical impairment identification.

1. Introduction

Epilepsy is more than epileptic seizures. It is a complex disease causing devastating effects on the quality of life for patients (Chang and Lowenstein, 2003). In the case of children with early-onset epilepsy (CWEEO; children with epilepsy onset < 5 years of age), the disease often co-occurs (up to 80%) with cognitive impairment (CI) which frequently and severely affect the quality of life for both the children and their families (Yoong, 2015). Preschool children with epilepsy also may be at increased risk of CI at ages where it is difficult and resource intensive to assess CI clinically for potential early intervention (Yoong, 2015). Therefore, there is a need to understand the causes of impairment in CWEEO and to find reliable, affordable and non-invasive markers that would help to decide therapeutic interventions beyond the current standard techniques.

The pathophysiology behind impairment (including autism and other learning difficulties) in CWEEO remains uncertain, particularly for preschool children (Yoong, 2015). Timely identification of CI is critical because early-life interventions are likely to be more effective (Bailey, 2001). Better understanding the risk factors and related markers to CI could provide the basis for novel interventions in CWEEO and improved public health strategies for primary and secondary prevention, concepts supported by recent calls to action (England et al., 2012).

Electroencephalography (EEG) is a non-invasive, portable and affordable tool for assessing brain activity routinely used in the assessment of children with suspected epilepsy. It uses electrodes on the scalp to measure the electrical field generated by neurons in the brain. EEG has also been an ideal candidate to help in the identification, understanding and monitoring of diverse brain conditions (Stam, 2014). In particular, spectral measures from the EEG, such as the power spectrum density (PSD), are often the basis for investigations, ranging from memory performance (Klimesch, 1999) to brain-computer interfaces (Nicolas-Alonso and Gomez-Gil, 2012). Throughout early-life and child development, however, these spectral profiles vary rapidly with the maturing brain (Matsuura et al., 1985; Marshall et al., 2002; Amador et al., 1989; Gasser et al., 1988). Network connectivity analysis helps mitigate these variations by offering

alternative metrics for understanding diverse brain conditions through the lens of well-established graph network connectivity properties (Stam and Reijneveld, 2007). This paper proposes to analyze EEG brain activity in CWEOE using connectivity network metrics directly to identify and explore potential markers related to CI.

Markers derived from EEG networks may relay relevant information about the cause of CI, with networks representing functional characterization profiles of these children. The severity of cognitive disturbances, in addition to outcomes of epilepsy surgery and disease duration, correlates with the extent of changes in functional networks (Stam, 2014). Network abnormalities appear in both ictal and interictal states (Stam, 2014), a phenomenon found not only in EEG but fMRI data as well (Vlooswijk et al., 2011). However, the majority of these studies have only focused on the evaluation of networks in adults (Stam, 2014). Our hypothesis is that similar background abnormalities on routine screening EEGs can be revealed in CWEOE, using advanced signal processing methods and that the extracted information may be predictive of cognitive impairment.

2. Methods

The data processing pipeline for each child is summarized in Figure 1.

2.1. Dataset

A retrospective analysis of a preschool cohort (< 5 years) was used for this study. The cohort studied was prospectively recruited from National Health Service (NHS) hospitals in Fife and Lothian as part of the NEUROPROFILES study (Hunter et al., 2015). All children recruited into NEUROPROFILES had face-to-face assessment by a trained psychologist (MH) using the Bayley-III (0-2.5 years) or WPPSI-III (2.5-5 years) instruments appropriate for participant age, followed soon by routine clinical EEG recordings. Of 64 children available, 13 were excluded from the study due to corrupted EEG data and inconsistent or incompatible EEG acquisition parameters, resulting in a dataset of $n = 51$ children. If multiple EEG recordings existed, only the first recording was selected for each child to avoid weighting results toward children with more recordings and to select from the same awake resting-state data across all children. From the baseline EEG used in assessment of the children with potential newly-diagnosed epilepsy, the standard 10-20 EEG data set-up and the reported clinical measures of cognitive development (e.g. Bayley-III and WPPSI-III) scores were used for analysis (Hunter et al., 2015). The cognitive measures were converted into a normalized z -score measure of intelligence, henceforth referred to as the metric z -int. Seizure activity was removed in pre-processing, and analysis was blinded to any treatment or seizure frequency information.

2.2. Pre-processing

Raw EEG was pre-processed in Matlab using the Fieldtrip toolbox (Oostenveld et al., 2011). Resting-state EEG data was split into 2 second long sub-trials,

and bandpass filtered between 0.5-45 Hz. Artefacts were rejected using manual and automatic rejection. Manual artefact rejection removed clear outliers in both trial and channel data based upon high variance values ($var > 10^6$). Muscle, jump and ocular artefacts were automatically rejected using strict rejection criteria based on Fieldtrip suggested values (z -value rejection level $r = 0.4$).

Classical frequency bands of interest used in adult EEG studies, e.g. delta/theta/etc., may not inherently correspond on a 1-to-1 basis to EEG of children (Marshall et al., 2002; Miskovic et al., 2015; Orekhova et al., 2006). Thus analysis of clean EEG data was calculated using a 'narrow band' approach, with 2-Hz wide band for frequencies of interest (e.g. 1-31 Hz). This method is similar to work by Miskovic et al. (Miskovic et al., 2015), and avoids possible age-related bias within grouping frequencies.

Data reduction can reduce redundant computational expenses and improve interpretation of results in studies. Averaging baseline data across all trials for each child, at each individual narrow band achieved this aim, while still providing an overall picture of the network.

2.3. Network Analysis

Processed data was analyzed via EEG graph analysis (for a review see Stam 2005 (Stam, 2005) and further reading (Stam and Reijneveld, 2007; Bullmore and Sporns, 2009; Cabral et al., 2014)). By directly examining the abstracted network metrics in small narrow bands, connectivity properties across ages can be compared directly as opposed to comparing shifting spectral frequencies. Graphs of the EEG functional network were constructed from the cross-spectrum of all EEG electrode pairs. This study investigates three connectivity analysis methods. First is the imaginary part of coherency (ICOH), used as a standard measure (Nolte et al., 2004). ICOH is well documented, providing direct measures of true brain interactions from EEG while eliminating self-interaction and volume conduction effects (Nolte et al., 2004). A weakness of ICOH, however, is its dependence on phase-delays, leading to optimal performance for specific phase differences and complete failure for others (Stam et al., 2007; Vinck et al., 2011; Haufe et al., 2013).

The phase-slope index (PSI) was also investigated (Nolte et al., 2008). The PSI examines causal relations between two sources for a signal of interest through exploiting phase differences which identify 'driving' versus 'receiving' sources and determining their average phase-slope (Nolte et al., 2008). Importantly, the PSI is equally sensitive to all phase differences from cross-spectral data (Nolte et al., 2008), but also allows for equal contributions from each.

The weighted phase-lag index (WPLI) was also included for analysis (Stam et al., 2007; Vinck et al., 2011). The original phase-lag index (PLI) (Stam et al., 2007) is a robust measure derived from the asymmetry of instantaneous phase differences between two signals, resulting in a measure less sensitive to volume conduction effects and independent of signal amplitudes (Stam et al., 2007). The weighted version of the PLI reduces sensitivity to uncorrelated noise and small perturbations which may affect the standard PLI by adding proportional weighting based on the imaginary component of the cross-spectrum (Vinck et al.,

2011). Both the PSI and WPLI help capture potential phase-sensitive connections present in EEG networks from related, but different, perspectives.

Two network filtering methods were used for each connectivity analysis technique: the Minimum Spanning Tree (MST) (Tewarie et al., 2015) and the Cluster-Span Threshold (CST) (Smith et al., 2015). The MST is an acyclic sub-network graph connecting all nodes (electrodes) of a graph while minimizing link weights (connectivity strength) (Tewarie et al., 2015). The MST is a standard network filtering technique common in graph analysis, with the drawback of excluding naturally occurring dense networks in the data due to its acyclic nature, thereby potentially losing information in EEG graph analysis (Smith et al., 2017).

In contrast, the CST is a network filtering technique which balances the proportion of cyclic ‘clustering’ (connected) and acyclic ‘spanning’ (unconnected) structures within a graph (Smith et al., 2015). This balance thus retains naturally occurring ‘loops’ which can reflect dense networks without potential information loss (Smith et al., 2017).

For each combination of filtering/connectivity analysis above (e.g. MST-ICOH, CST-ICOH, MST-PSI, etc.) four network metrics were investigated for correlation to the z -int. Investigators pre-emptively selected network metrics prior to analysis, while blinded to the cognition status and clinical history of the subjects, to help reduce potential selection bias. The metrics were chosen to account for different network properties (e.g. the shape of the network, the critical connection points in the network etc.) with (relatively) little inter-correlation. Network metrics differ for MST and CST filtering due to the natural exclusion/inclusion of cycles, respectively. However, metrics across filters were selected to be comparable regarding network properties. Pictorial examples of the selected network metrics, alongside their short definitions, are outlined in Figure 2.

2.4. Statistical Analysis

Statistical analysis was done using Matlab 2015a. Correlation between individual network metrics and the z -int was measured using Kendall’s tau (τ) (Gilpin, 1993). Kendall’s τ calculates the difference between concordant and discordant pairs (Gilpin, 1993; Shong, 2010), and is ideal for describing ordinal or ranking properties, like the normalized z -int. Its design is also relatively robust to false positive correlations from data outliers (Gilpin, 1993; Shong, 2010), providing additional mitigation to spurious correlations in the results.

Correlation trends in this work are reported as the uncorrected $p < 0.05\%$ values, with the condition that correlations considered potentially significant under the assumption of family dependencies across frequency bins are to be noted by the \dagger symbol for Bonferroni corrections, similar in style to previous literature (Fraga González et al., 2016). For completeness, a full list of all uncorrected τ and corresponding p -values in this study are also included in the supporting information in a spreadsheet format.

163 2.5. Classification

164 A multi-class classification scheme was devised using the Weka toolbox (Hall
165 et al., 2009; Frank et al., 2016). Class labels of *normal*, *mild/moderate*, and *se-*
166 *vere* cognitive impairment were chosen for z -int within ± 1 standard deviation
167 (S.D.), between -1 to -2 S.D. and over -2 S.D. from the norm, respectively.
168 Primary feature selection included all correlations identified by the statistical
169 analysis, to help retain interpretation of resulting network features. Then,
170 a second feature selection phase using nested 5-fold cross-validation selected
171 prominent features via bi-directional subspace evaluation (Khalid et al., 2014).
172 Within this nested cross-validation, features identified as important in $> 70\%$
173 of the folds were selected for use in classification.

174 Due to the natural skew of the data (towards normalcy), and the context
175 of the classification problem (e.g. misclassifying different classes has various
176 implications), a cost-sensitive classifier was developed (Zhou and Liu, 2010). In
177 order to properly develop such a classifier, an appropriate cost matrix needed
178 to be identified. Using guidelines outlined in literature (Zhou and Liu, 2010),
179 the cost matrix in Table 1 was developed, with predicted classes on the rows
180 and real classes on the columns.

181 The defined matrix satisfies several key concerns in multi-class cost-matrix
182 development (Zhou and Liu, 2010). The weights on misclassification were care-
183 fully selected to reflect probable clinical concerns in classification with guidance
184 from a paediatric neurologist. The cost for incorrectly classifying an impaired
185 child as normal is twice as heavy compared to misclassifying a normal child
186 into either impaired group, which is still significantly more punishing than cor-
187 rectly identifying impairment and only misclassifying between mild/moderate
188 or severe impairments. These weighted values prioritize correctly including as
189 many ‘true positive’ children with CI, i.e. increasing sensitivity, followed by a
190 secondary prioritization upon being able to discern the level of CI. These bound-
191 aries provide a more clinically relevant classification context in the analysis.

192 Using the selected features and developed cost-sensitive matrix, a nested
193 5-fold cross-validation trained a simple K -Nearest Neighbour (KNN) classifier,
194 with $N = 3$ neighbours and Euclidean distance to minimize the above costs. A
195 repeated ‘bagging’ (Bootstrap Aggregation (Shao, 1996)) approach was used to
196 reduce variance in the classifier at a rate of 100 iterations/fold. Results were
197 evaluated upon their overall classification accuracy and total penalty costs (e.g.
198 sum of all mistakes based on the cost matrix). Random classification and naive
199 classification (e.g. only choosing a single class for all subjects) was included for
200 comparison.

201 3. Results

202 3.1. Correlation Analysis

203 Each combination of network analysis (ICOH/PSI/WPLI) and filtering (MST/CST)
204 techniques uncovered likely correlations between at least one network metric

(outlined in Figure 2) and the z -int representing CI. A summary of the significant correlations between the MST metrics and z -int scores are shown in Table 2. All MST correlations were in the medium to high frequency range, 9 – 31 Hz, with no significant results in lower frequencies. Activity above approximately 9 Hz is outside of the expected range for the delta, theta and alpha bands in young children (Marshall et al., 2002; Orekhova et al., 2006). Sets of contiguous frequency bands with significant correlations were found in the ICOH and PSI connectivity measures, and are reported together as a single frequency range. Overlapping correlations retained at significant levels after partial correlation correcting for age are also reported for the MST using a modified Kendall’s τ .

Similarly, significant correlations between the CST metrics and z -int are shown in Table 3. Several significant CST metrics exist in the lower frequency range (< 9 Hz), indicating a potential sensitivity of the CST to lower frequencies. No sets of continuous frequency bands were discovered, but several sets were trending towards this phenomenon within ICOH. Multiple overlapping correlations remaining after partial correlation correction for age from the modified τ in the CST at lower frequencies indicate additional sensitivity.

Both the MST and CST demonstrate high sensitivity in the phase-dependent measures (PSI, WPLI) compared to the standard ICOH.

3.2. KNN Classification

Based upon the possible sensitivity of the CST, a preliminary classification scheme assessed the potential predictive qualities of the CST network metrics in identifying CI classes. The relative quality of the classifications are examined using classification accuracy and total ‘cost’ (i.e. penalty for misidentification) (Zhou and Liu, 2010).

The subset of CST metrics for classification, identified from significant correlations and chosen via cross-validated feature selection, included five network metrics across the three connectivity measures. For ICOH, the identified subset selected was the betweenness centrality at ranges 11-13 and 19-21 Hz alongside the clustering coefficient at a range of 15-17 Hz. The subset also included the PSI average degree at 13-15 Hz and the WPLI variance degree from 1-3 Hz. These results indicate specifically which network metrics, from a machine-learning perspective, contributed the most information for building an accurate classification model.

The resulting confusion matrix from the 5-fold cross-validated, cost-sensitive classification analysis is seen in Table 4.

The overall classification accuracy was 70.5% with a total ‘cost-penalty’, based on Table 1, of 38 points. The expected random classification accuracy is based on the distribution of individuals belonging to each class, i.e. 31, 7 and 13 children for the *normal*, *mild/moderate* and *severe* classes respectively. Random accuracy would be expected at 45.4%, with cost-penalty varying depending on misclassification distributions. Using the average misclassification penalty and the percentage of children who would be misidentified (approximately 23 of the 51 subjects), the cost-penalty would be at least 65 points. Naive classification

assumes all subjects belong to a single class only. Selecting for the normal, mild/moderate and severe classes provides classification accuracies of 60.8%, 13.7%, and 25.5% respectively. Similarly, the total cost-penalty for each naive classification would be 100, 90.5 and 84.5 points respectively. The results indicate gains in classification accuracy and a reduced total penalty as compared to both random and naive classification.

Using 5-fold cross-validation, the results provide a decent classification on two tiers. First, the proposed classifier is able to generally identify cognitively normal from impaired children (both mild/moderate and severe). Of all impaired children, only three are misidentified as within the normal range, giving a sensitivity of 85%, while only five normal children are misidentified as generally impaired (either mild/moderate or severe), giving a specificity of approximately 84%. The second tier of the classifier attempts to separate out cases of mild/moderate impairment from severe impairment. Despite being less well defined than the general case, the simple classifier is still able to identify > 50% of the remaining cases as the correct impairment. Improving this second tier of classification through more complex methods is a consideration for future work.

4. Discussion

This paper aimed to describe a new set of techniques based on signal and network analysis for identifying possible markers of cognitive impairment in preschool children with epilepsy. Although the exact reason for CI in epilepsy is less well understood, clinical observations and investigations indicate it is likely multifactorial, based upon underlying aetiology, seizure type and frequency, EEG background, etc., with variations relating to the severity of CI within these categories. Early identification of CI is critical but difficult for preschool children compared to older children with epilepsy, as school settings may provide easier recognition of CI. EEG network analysis as a tool thus may help predict CI better within these groups for preschool children, which in turn help clinicians inform parents and target early interventions.

The proposed methodology represents a scientifically sound and clinically relevant option for characterizing networks of interest reflecting CI in CWEOE. The results indicate a substantial pool of potential characteristics might be identified using the proposed methods with several network analysis and filtering combinations. The breadth of these combinations emphasizes the general suitability of networks in identifying possible cognitive impairment markers in CWEOE, and demonstrates for the first time preliminary identification of such profiles in preschool children.

Flexibility in sensitivity and robustness of particular networks to features of interest is an advantage of this analysis. For instance, the sensitivity of phase-dependent connectivity measures, e.g. PSI and WPLI, was more prevalent compared to standard ICOH. This is not surprising as phase-oriented measures were developed to improve upon phase ambiguities in traditional ICOH measurements (Nolte et al., 2008; Haufe et al., 2013). In addition, the sensitivity of PSI in picking up significant correlations can be attributed in part to its equal

treatment of small phase differences in leading and lagging signals (Nolte et al., 2008). Such small phase differences contribute equally in PSI, while counting for proportionally less in the WPLI by definition (Vinck et al., 2011; Stam et al., 2007). By construction, the WPLI results are substantially more robust to noise and small perturbations in phase, through proportionally reflecting phase differences in network connections with appropriate weights, providing results for only large phase differences. Together these measures reflect trade-off choices between sensitivity and robustness for network analysis.

Of interest for paediatric populations is the CST's capability to identify low frequency correlations in phase-dependent coherency measures. Both the PSI and WPLI demonstrate sensitivity to lower frequencies, not present in the ICOH or MST in general. This is critical considering that in preschool children lower frequencies typically contain the bands of interest present in adult EEGs, e.g. the delta/theta/alpha bands (Marshall et al., 2002; Orekhova et al., 2006). During development these bands shift to higher frequencies (Chiang et al., 2011), reflecting a large scale reorganization of the endogenous brain electric fields and suggesting a transition to more functionally integrated and coordinated neuronal activity (Miskovic et al., 2015). The (low) chance of all such significant findings being spurious is of less detriment than the potential loss of impact for disregarding the findings if at least one of them is true. The sensitivity to detect network disruptions already present in these critical bands in CWEOE provide high value in adjusting potential therapeutic and treatment strategies for clinicians.

The identified subset of metrics for classification provide additional information. All of the features in the subset reflected distribution measures of hub-like network structures in the brain, relating to the balance between heterogeneity and centrality within the network. The implicated metrics, other than the variance degree, corresponded to measures identifying local, centralized 'critical' nodes in a network. Their negative correlation to the z -int imply that children with more locally centralized brain networks, and consequently with less well distributed hub-like structures, are more likely to have corresponding cognitive impairment. This is reasonable, since if there exists a small set of central, critical hubs responsible for communication across the brain, disruption of these critical points (e.g. due to seizure activity) would have severely negative effects on communication connections. This is also supported by the negative correlation in the variance degree metric in the WPLI. The variance degree can be interpreted as a measure of a network's heterogeneity (Snijders, 1981). As such, the negative variance degree in the low (1-3 Hz) frequency range may reflect stunted cognitive development, as normal maturation is associated with reduced activation in low frequencies (Matsuura et al., 1985; Marshall et al., 2002; Amador et al., 1989; Orekhova et al., 2006; Gasser et al., 1988), implying a decrease in local connectivity and heterogeneity of the networks. This compliments the above conclusions, suggesting a sensitivity in the likely well-centralized networks to significant disruptions by epilepsy. The disrupted networks may then be reflected by the continued heterogeneity and local connectivity of low frequency structures in impaired children.

Furthermore, being able to predict the likely degree of cognitive impairment using the identified markers could provide an additional tool for clinicians. Specifically, being able to pair specific network features to an effective prediction of CI would allow clinicians to retain the interpretability of the chosen network features while providing a tool to quickly and objectively separate similar cases. To this end, the cost-sensitive, simple KNN classifier explored in this work illustrates a primitive step towards this aim. The proposed classifier and associated methods provide considerable results of approximately 85% and 84% sensitivity and specificity, respectively, to general impairment while still relatively accurately separating sub-classifications of impairment.

The automated nature of the processing chain and its use of routinely acquired EEG data makes the proposed methods an attractive proposition for clinical applications. The NEUROPROFILE cohort was advantageous in that formal neuropsychological testing was coupled with EEG recordings, making it ideal for this investigation. Future work could include alternative narrow-band frequency binning and less strict automated rejection methods. Significant correlations across sets of consecutive (and nearly consecutive) frequency bands indicate likely targets for potential follow-up studies. Further development of a more complex classification scheme could help improve the second tier separation of cognitive impairment types (e.g. mild/moderate from severe). Investigations into correlations to brain abnormalities on MRI could also provide additional validation of the results. Replication of these methods using another large dataset may also bolster the generalizability of the techniques.

4.1. Limitations

There are limitations associated with these results. Although this novel study used routine clinical EEGs used in the diagnosis of incidence cases of early onset epilepsy, the three classes of normal, mild/moderate and severe impairment were unbalanced; this occurred naturally. The majority of the sample was taken from a population-based cohort, and mitigating potential influences from imbalanced data was taken into account as much as possible when conducting the research, e.g. through cost-sensitive analysis. Imbalanced data is not uncommon, and the unbalanced distribution of CI may reflect findings in a population-based sample, i.e. the full NEUROPROFILES data (Hunter et al., 2015).

Also, although all the patients had early onset epilepsy (i.e. before five years of age), the epilepsy type and aetiologies were heterogenous. Thus we are unable to determine if the model and methods used have greater or lesser predictive value in specific subsets. Testing in a larger, more homogeneous sample would provide clarification.

5. Conclusions

This study introduced a novel processing chain based on network analysis for identifying markers of cognitive impairment in preschool CWOE for the first

time. Results from the study demonstrate these network markers in identifying critical structures of CWEOE with CI and illustrate their potential predictive abilities using preliminary classification techniques.

6. Acknowledgements

The authors would like to thank the patients and families who participated in the NEUROPROFILES (Hunter et al., 2015) study. Funding support for this project was provided by the RS McDonald Trust, Thomas Theodore Scott Ingram Memorial Fund, and the Muir Maxwell Trust.

7. Author Contributions

Javier Escudero and Richard FM Chin conceived of the presented ideas. Eli Kinney-Lang developed the theory, performed data analysis and interpretation, and designed the computational framework of the project under supervision of Richard FM Chin and Javier Escudero. Jay Shetty, Krishnaraya Kamath Tallur, Michael Yoong and Ailsa McLellan were involved in the methodology and collection of the original NEUROPROFILES dataset, including recruiting patients and requesting and reporting patient EEGs. Matthew Hunter was the lead author and investigator for the NEUROPROFILES project with senior supervision under Richard FM Chin. Eli Kinney-Lang wrote the manuscript and figures, with revision and comments provided by Matthew Hunter, Michael Yoong, Jay Shetty, Krishnaraya Kamath Tallur, Ailsa McLellan, Richard FM Chin and Javier Escudero. Final approval of this publication was provided by all authors.

Conflict of Interest Statement

None of the authors have potential conflicts of interest to be disclosed.

References

- Amador, A., Valdés Sosa, P., Pascual Marqui, R., Garcia, L., Lirio, R., Bayard, J., Jul. 1989. On the structure of EEG development. *Electroencephalogr. Clin. Neurophysiol.* 73 (1), 10–19.
URL <http://linkinghub.elsevier.com/retrieve/pii/0013469489900151>
- Bailey, D. B., 2001. Critical thinking about critical periods.
- Bullmore, E., Sporns, O., Mar. 2009. Complex brain networks: graph theoretical analysis of structural and functional systems. *Nat. Rev. Neurosci.* 10 (4), 312–312.
URL <http://www.nature.com/doi/10.1038/nrn2618>

- 416 Cabral, J., Kringelbach, M. L., Deco, G., 2014. Exploring the network dynamics
417 underlying brain activity during rest. *Prog. Neurobiol.* 114, 102–131.
418 URL <http://dx.doi.org/10.1016/j.pneurobio.2013.12.005>
- 419 Chang, B. S., Lowenstein, D. H., 2003. *Epilepsy*. *N. Engl. J. Med.* 349, 1257–
420 1266.
- 421 Chiang, A., Rennie, C., Robinson, P., van Albada, S., Kerr, C., 2011. Age
422 trends and sex differences of alpha rhythms including split alpha peaks. *Clin.*
423 *Neurophysiol.* 122 (8), 1505–1517.
424 URL [http://linkinghub.elsevier.com/retrieve/pii/](http://linkinghub.elsevier.com/retrieve/pii/S1388245711000903)
425 [S1388245711000903](http://linkinghub.elsevier.com/retrieve/pii/S1388245711000903)
- 426 England, M. J., Liverman, C. T., Schultz, A. M., Strawbridge, L. M., 2012.
427 *Epilepsy across the spectrum: Promoting health and understanding. A sum-*
428 *mary of the Institute of Medicine report.*
- 429 Fraga González, G., Van der Molen, M., Žarić, G., Bonte, M., Tijms, J.,
430 Blomert, L., Stam, C., Van der Molen, M., 2016. Graph analysis of EEG
431 resting state functional networks in dyslexic readers. *Clin. Neurophysiol.*
432 127 (9), 3165–3175.
433 URL [http://linkinghub.elsevier.com/retrieve/pii/](http://linkinghub.elsevier.com/retrieve/pii/S1388245716304539)
434 [S1388245716304539](http://linkinghub.elsevier.com/retrieve/pii/S1388245716304539)
- 435 Frank, E., Hall, M. A., Witten, I. H., 2016. The WEKA Workbench. In:
436 Morgan Kaufmann, Fourth Ed. pp. 553–571.
437 URL [http://www.cs.waikato.ac.nz/ml/weka/Witten_et_al_2016_](http://www.cs.waikato.ac.nz/ml/weka/Witten_et_al_2016_appendix.pdf)
438 [appendix.pdf](http://www.cs.waikato.ac.nz/ml/weka/Witten_et_al_2016_appendix.pdf)
- 439 Gasser, T., Verleger, R., Bächer, P., Sroka, L., Feb. 1988. Development of
440 the EEG of school-age children and adolescents. I. Analysis of band power.
441 *Electroencephalogr. Clin. Neurophysiol.* 69 (2), 91–99.
442 URL [http://linkinghub.elsevier.com/retrieve/pii/](http://linkinghub.elsevier.com/retrieve/pii/S0013469488902040)
443 [S0013469488902040](http://linkinghub.elsevier.com/retrieve/pii/S0013469488902040)
- 444 Gilpin, A. R., Mar. 1993. Table for Conversion of Kendall’s Tau to Spearman’s
445 Rho Within the Context of Measures of Magnitude of Effect for Meta-
446 Analysis. *Educ. Psychol. Meas.* 53 (1), 87–92.
447 URL [http://epm.sagepub.com/cgi/doi/10.1177/](http://epm.sagepub.com/cgi/doi/10.1177/0013164493053001007)
448 [0013164493053001007](http://epm.sagepub.com/cgi/doi/10.1177/0013164493053001007)[http://journals.sagepub.com/doi/10.1177/](http://journals.sagepub.com/doi/10.1177/0013164493053001007)
449 [0013164493053001007](http://journals.sagepub.com/doi/10.1177/0013164493053001007)
- 450 Hall, M., Frank, E., Holmes, G., Pfahringer, B., Reutemann, P., Witten, I. H.,
451 2009. The WEKA data mining software. *ACM SIGKDD Explor.* 11 (1),
452 10–18.
453 URL [http://portal.acm.org/citation.cfm?doid=1656274.1656278\\$](http://portal.acm.org/citation.cfm?doid=1656274.1656278%delimter%026E30F$npapers2://publication/doi/10.1145/1656274.1656278)
454 [delimter"026E30F\\$npapers2://publication/doi/10.1145/1656274.](http://portal.acm.org/citation.cfm?doid=1656274.1656278%delimter%026E30F$npapers2://publication/doi/10.1145/1656274.1656278)
455 [1656278](http://portal.acm.org/citation.cfm?doid=1656274.1656278%delimter%026E30F$npapers2://publication/doi/10.1145/1656274.1656278)

- 456 Haufe, S., Nikulin, V. V., Müller, K.-R., Nolte, G., Jan. 2013. A critical
457 assessment of connectivity measures for EEG data: A simulation study.
458 Neuroimage 64 (1), 120–133.
459 URL <http://dx.doi.org/10.1016/j.neuroimage.2012.09.036><http://linkinghub.elsevier.com/retrieve/pii/S1053811912009469>
460
- 461 Hunter, M., Sumpter, R., Verity, K., Yoong, M., McLellan, A., Shetty, J., Chin,
462 R., 2015. Neurodevelopment in preschool children of fife and lothian epilepsy
463 study: Neuroprofiles-a population-based study. Developmental Medicine &
464 Child Neurology 57, 56–57.
- 465 Khalid, S., Khalil, T., Nasreen, S., Aug. 2014. A survey of feature selection and
466 feature extraction techniques in machine learning. In: 2014 Sci. Inf. Conf.
467 IEEE, pp. 372–378.
468 URL [http://ieeexplore.ieee.org/lpdocs/epic03/wrapper.htm?](http://ieeexplore.ieee.org/lpdocs/epic03/wrapper.htm?arnumber=6918213)
469 [arnumber=6918213](http://ieeexplore.ieee.org/lpdocs/epic03/wrapper.htm?arnumber=6918213)
- 470 Klimesch, W., 1999. EEG alpha and theta oscillations reflect cognitive and
471 memory performance: A review and analysis.
- 472 Marshall, P. J., Bar-Haim, Y., Fox, N. A., 2002. Development of the EEG from
473 5 months to 4 years of age. Clin. Neurophysiol. 113 (8), 1199–1208.
474 URL [http://www.sciencedirect.com/science/article/pii/](http://www.sciencedirect.com/science/article/pii/S1388245702001633)
475 [S1388245702001633](http://www.sciencedirect.com/science/article/pii/S1388245702001633)
- 476 Matsuura, M., Yamamoto, K., Fukuzawa, H., Okubo, Y., Uesugi, H., Moriiwa,
477 M., Kojima, T., Shimazono, Y., 1985. Age development and sex differences
478 of various EEG elements in healthy children and adults—quantification by a
479 computerized wave form recognition method. Electroencephalogr Clin Neu-
480 rophysiol 60 (5), 394–406.
481 URL <http://www.ncbi.nlm.nih.gov/pubmed/2580690>
- 482 Miskovic, V., Ma, X., Chou, C.-A., Fan, M., Owens, M., Sayama, H., Gibb,
483 B. E., Sep. 2015. Developmental changes in spontaneous electrocortical
484 activity and network organization from early to late childhood. Neuroimage
485 118, 237–47.
486 URL [http://linkinghub.elsevier.com/retrieve/pii/](http://linkinghub.elsevier.com/retrieve/pii/S1053811915005108)
487 [S1053811915005108](http://linkinghub.elsevier.com/retrieve/pii/S1053811915005108)[http://dx.doi.org/10.1016/j.neuroimage.](http://dx.doi.org/10.1016/j.neuroimage.2015.06.013)
488 [2015.06.013](http://dx.doi.org/10.1016/j.neuroimage.2015.06.013)[http://www.sciencedirect.com/science/article/](http://www.sciencedirect.com/science/article/pii/S1053811915005108)
489 [pii/S1053811915005108](http://www.sciencedirect.com/science/article/pii/S1053811915005108)[http://www.ncbi.nlm.nih.gov/pubmed/](http://www.ncbi.nlm.nih.gov/pubmed/26057595)
490 [26057595](http://www.ncbi.nlm.nih.gov/pubmed/26057595)<http://www.pubmedcentral.nih.gov>
- 491 Nicolas-Alonso, L. F., Gomez-Gil, J., 2012. Brain computer interfaces, a review.
492 Sensors (Basel). 12 (2), 1211–79.
493 URL www.mdpi.com/journal/sensors<http://www.ncbi.nlm.nih.gov/pubmed/22438708>[http://www.pubmedcentral.nih.gov/articlerender.](http://www.pubmedcentral.nih.gov/articlerender.fcgi?artid=PMC3304110)
494 [fcgi?artid=PMC3304110](http://www.pubmedcentral.nih.gov/articlerender.fcgi?artid=PMC3304110)
495

- 496 Nolte, G., Bai, O., Wheaton, L., Mari, Z., Vorbach, S., Hallett, M., 2004.
497 Identifying true brain interaction from EEG data using the imaginary part of
498 coherency. Clin. Neurophysiol. 115 (10), 2292–2307.
- 499 Nolte, G., Ziehe, A., Nikulin, V. V., Schlögl, A., Krämer, N., Brismar, T.,
500 Müller, K.-R., Jun. 2008. Robustly Estimating the Flow Direction of Infor-
501 mation in Complex Physical Systems. Phys. Rev. Lett. 100 (23), 234101.
502 URL <https://link.aps.org/doi/10.1103/PhysRevLett.100.234101>
- 503 Oostenveld, R., Fries, P., Maris, E., Schoffelen, J. M., 2011. FieldTrip: Open
504 source software for advanced analysis of MEG, EEG, and invasive electro-
505 physiological data. Comput. Intell. Neurosci. 2011.
- 506 Orekhova, E. V., Stroganova, T. A., Posikera, I. N., Elam, M., 2006. EEG
507 theta rhythm in infants and preschool children. Clin. Neurophysiol. 117 (5),
508 1047–1062.
509 URL [http://linkinghub.elsevier.com/retrieve/pii/
510 S1388245706000095](http://linkinghub.elsevier.com/retrieve/pii/S1388245706000095)
- 511 Shao, J., 1996. Bootstrap Model Selection. J. Am. Stat. Assoc. 91 (434),
512 655–665.
513 URL [http://www.jstor.org/stable/2291661\\$\\
514 delimiter\"026E30F\\$nhhttps://www.jstor.org/stable/pdfplus/10.
515 2307/2291661.pdf?acceptTC=true](http://www.jstor.org/stable/2291661$\\delimitter\)
- 516 Shong, N., 2010. Pearsons versus Spearmans and Kendalls correlation coeffi-
517 cients for continuous data. Ph.D. thesis.
- 518 Smith, K., Abasolo, D., Escudero, J., 2017. Accounting for the complex hi-
519 erarchical topology of EEG phase-based functional connectivity in network
520 binarisation. PLoS One.
- 521 Smith, K., Azami, H., Parra, M. A., Starr, J. M., Escudero, J., 2015. Cluster-
522 span threshold: An unbiased threshold for binarising weighted complete net-
523 works in functional connectivity analysis. Proc. Annu. Int. Conf. IEEE Eng.
524 Med. Biol. Soc. EMBS 2015-Novem, 2840–2843.
- 525 Snijders, T. A., Jan. 1981. The degree variance: An index of graph heterogene-
526 ity. Soc. Networks 3 (3), 163–174.
527 URL [http://linkinghub.elsevier.com/retrieve/pii/
528 0378873381900149](http://linkinghub.elsevier.com/retrieve/pii/0378873381900149)
- 529 Stam, C. J., Oct. 2005. Nonlinear dynamical analysis of EEG and MEG:
530 Review of an emerging field.
531 URL [http://linkinghub.elsevier.com/retrieve/pii/
532 S1388245705002403](http://linkinghub.elsevier.com/retrieve/pii/S1388245705002403)
- 533 Stam, C. J., 2014. Modern network science of neurological disorders. Nat. Rev.
534 Neurosci. 15 (10), 683–695.
535 URL <http://www.nature.com/doifinder/10.1038/nrn3801>

536 Stam, C. J., Nolte, G., Daffertshofer, A., 2007. Phase lag index: Assessment of
537 functional connectivity from multi channel EEG and MEG with diminished
538 bias from common sources. *Hum. Brain Mapp.* 28 (11), 1178–1193.

539 Stam, C. J., Reijneveld, J. C., 2007. Graph theoretical analysis of complex
540 networks in the brain. *Nonlinear Biomed. Phys.* 1 (1), 3.
541 URL [http://nonlinearbiomedphys.biomedcentral.com/articles/10.](http://nonlinearbiomedphys.biomedcentral.com/articles/10.1186/1753-4631-1-3)
542 [1186/1753-4631-1-3](http://nonlinearbiomedphys.biomedcentral.com/articles/10.1186/1753-4631-1-3)

543 Tewarie, P., van Dellen, E., Hillebrand, A., Stam, C. J., 2015. The minimum
544 spanning tree: An unbiased method for brain network analysis. *Neuroimage*
545 104, 177–188.
546 URL <http://dx.doi.org/10.1016/j.neuroimage.2014.10.015>

547 Vinck, M., Oostenveld, R., Van Wingerden, M., Battaglia, F., Pennartz, C.
548 M. A., 2011. An improved index of phase-synchronization for electrophysio-
549 logical data in the presence of volume-conduction, noise and sample-size bias.
550 *Neuroimage* 55 (4), 1548–1565.
551 URL <http://dx.doi.org/10.1016/j.neuroimage.2011.01.055>

552 Vlooswijk, M., Vaessen, M. J., Jansen, J., De Krom, M., Majoie, H., Hofman, P.,
553 Aldenkamp, A. P., Backes, W. H., 2011. Loss of network efficiency associated
554 with cognitive decline in chronic epilepsy. *Neurology* 77 (10), 938–944.

555 Yoong, M., Apr. 2015. Quantifying the deficit-imaging neurobehavioural
556 impairment in childhood epilepsy. *Quant. Imaging Med. Surg.* 5 (2), 225–37.
557 URL <http://www.ncbi.nlm.nih.gov/pubmed/25853081>[http://www.](http://www.pubmedcentral.nih.gov/articlerender.fcgi?artid=PMC4379313/pmc/articles/PMC4379313/?report=abstract)
558 [pubmedcentral.nih.gov/articlerender.fcgi?artid=PMC4379313/pmc/](http://www.pubmedcentral.nih.gov/articlerender.fcgi?artid=PMC4379313/pmc/articles/PMC4379313/?report=abstract)
559 [articles/PMC4379313/?report=abstract](http://www.pubmedcentral.nih.gov/articlerender.fcgi?artid=PMC4379313/pmc/articles/PMC4379313/?report=abstract)

560 Zhou, Z.-H., Liu, X.-Y., 2010. On multi-class cost-sensitive learning. *Comput.*
561 *Intell.* 26 (3), 232–257.
562 URL [https://www.scopus.com/inward/record.uri?eid=2-s2.](https://www.scopus.com/inward/record.uri?eid=2-s2.0-77955034751&doi=10.1111/j.1467-8640.2010.00358.x&partnerID=40&md5=21d7f85735dd6b67beeb0f73e6177cf7)
563 [0-77955034751&doi=10.1111/j.1467-8640.2010.00358.x&partnerID=](https://www.scopus.com/inward/record.uri?eid=2-s2.0-77955034751&doi=10.1111/j.1467-8640.2010.00358.x&partnerID=40&md5=21d7f85735dd6b67beeb0f73e6177cf7)
564 [40&md5=21d7f85735dd6b67beeb0f73e6177cf7](https://www.scopus.com/inward/record.uri?eid=2-s2.0-77955034751&doi=10.1111/j.1467-8640.2010.00358.x&partnerID=40&md5=21d7f85735dd6b67beeb0f73e6177cf7)

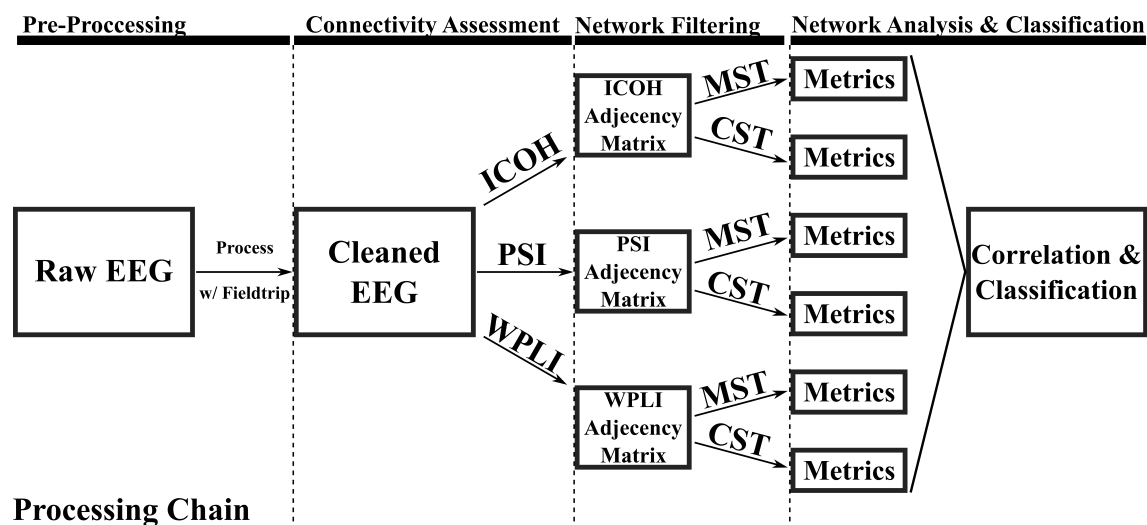
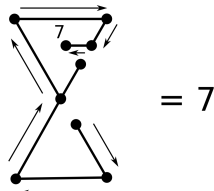
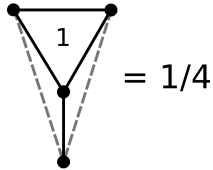
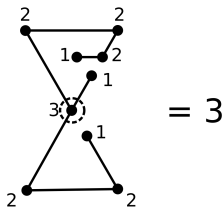
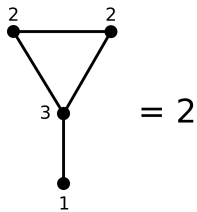
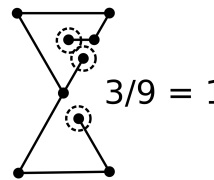
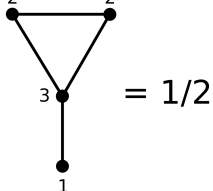
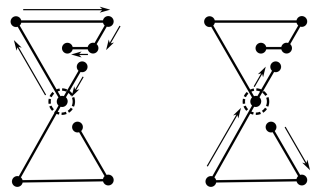
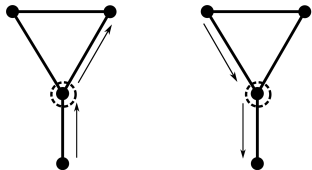


Figure 1: Flowchart of data processing chain for an individual child. ICOH = Imaginary part of coherency, PSI = Phase-slope index, WPLI = Weighted phase-lag index, MST = Minimum Spanning Tree, CST = Cluster-Span Threshold

Figure 2: Illustration of all graph analysis metrics for the Minimum Spanning Tree (MST) and Cluster-Span Threshold (CST) networks using simple example graphs. Nodes (dots) represent EEG channel electrodes. Edges (lines) represent functional interactions between EEG channels identified by a connectivity measure, e.g. ICOH/PSI/WPLI.

MST	CST
<p>Diameter: The longest 'shortest path' from any two nodes</p>  <p>= 7</p>	<p>Clustering Coefficient: Formed 'clustering' triangles out of all possible triangle clusters (max)</p>  <p>= 1/4</p>
<p>Max Degree: The node with the largest number of connecting edges</p>  <p>= 3</p>	<p>Average Degree: The average degree of all graph nodes</p>  <p>= 2</p>
<p>Leaf Fraction: The fraction of the total nodes with degree = 1</p>  <p>$3/9 = 1/3$</p>	<p>Variance Degree: The variance of all degree values in a graph</p>  <p>= 1/2</p>
<p>Betweenness Centrality: Measures 'centrality' of nodes with respect to various shortest paths</p> 	<p>Betweenness Centrality: Measures 'centrality' of nodes with respect to various shortest paths</p> 

Multi-class Classification Cost Matrix				
		CI-Predicted Class		
		Normal	Mild/Mod.	Severe
CI-True Class	Normal	0	2.5	2.5
	Mild/Mod.	5	0	1
	Severe	5	1	0

Table 1: Weighted cost matrix for misclassification of cognitive impairment (CI) for normal (± 1 SD), mild/moderate (-1 to -2 SD) and severe (< -2 SD) classes. Rows represent true class labels, with columns as the predicted classification labels.

MST analysis of z -int score			
Network Type	Network Measurement	Frequency Range(s) (Hz)	Correlation ($\bar{\tau} \pm SD$)
ICOH	Diameter	—	—
ICOH	Maximum Degree	—	—
ICOH	Leaf Fraction	—	—
ICOH	Betweenness Centrality	13-17 Hz	-0.231 ± 0.001
PSI	Diameter	9-19 Hz	$0.239 \pm 0.032^{\dagger*}$
PSI	Maximum Degree	11-13 Hz	$-0.232 \pm 0.000^*$
PSI	Maximum Degree	15-17 Hz	$-0.258 \pm 0.000^{\dagger*}$
PSI	Maximum Degree	21-23 Hz	-0.219 ± 0.000
PSI	Leaf Fraction	11-13 Hz	-0.201 ± 0.000
PSI	Leaf Fraction	15-19 Hz	-0.246 ± 0.003
PSI	Betweenness Centrality	9-13 Hz	$-0.218 \pm 0.012^*$
PSI	Betweenness Centrality	17-19 Hz	$-0.259 \pm 0.000^{\dagger*}$
WPLI	Diameter	—	—
WPLI	Maximum Degree	29-31 Hz	$-0.310 \pm 0.000^{\dagger*}$
WPLI	Leaf Fraction	—	—
WPLI	Betweenness Centrality	23-25 Hz	0.223 ± 0.000

Table 2: Summary of Kendall's τ correlation trends between various graph metrics and the z -int score using the Minimum Spanning Tree (MST). For all values $|\tau|$ was between 0.201 and 0.310; mean = 0.239 ± 0.0278 and uncorrected $p < 0.05$. Significant values across contiguous narrow-band frequencies have been grouped together for ease of interpretation.

† Significant with Bonferroni correction at the level of frequencies.

* Significant after partial correlation correction to age of subjects, via modified τ with uncorrected $p < 0.05$.

CST analysis of z -int score			
Network Type	Network Measurement	Frequency Range(s) (Hz)	Correlation ($\bar{\tau} \pm SD$)
ICOH	Clustering Coefficient	15-17 Hz	$-0.290 \pm 0.000^{\dagger*}$
ICOH	Average Degree	—	—
ICOH	Variance of Degree	13-15 Hz	-0.200 ± 0.000
ICOH	Variance of Degree	21-23 Hz	-0.203 ± 0.000
ICOH	Betweenness Centrality	11-13 Hz	$-0.273 \pm 0.000^{\dagger*}$
ICOH	Betweenness Centrality	15-17 Hz	-0.241 ± 0.000
ICOH	Betweenness Centrality	19-21 Hz	-0.203 ± 0.000
PSI	Clustering Coefficient	—	—
PSI	Average Degree	13-15 Hz	-0.210 ± 0.000
PSI	Variance of Degree	15-17 Hz	$-0.277 \pm 0.000^{\dagger*}$
PSI	Variance of Degree	21-23 Hz	-0.217 ± 0.000
PSI	Betweenness Centrality	5-7 Hz	$0.204 \pm 0.000^*$
PSI	Betweenness Centrality	15-17 Hz	-0.248 ± 0.000
WPLI	Clustering Coefficient	1-3 Hz	$-0.236 \pm 0.000^*$
WPLI	Clustering Coefficient	17-19 Hz	$0.287 \pm 0.000^{\dagger*}$
WPLI	Average Degree	—	—
WPLI	Variance of Degree	1-3 Hz	$-0.236 \pm 0.000^*$
WPLI	Betweenness Centrality	—	—

Table 3: Summary of Kendall's τ correlation trends between various graph metrics and the z -int score using the Cluster-Span Threshold (CST). For all values $|\tau|$ was between 0.201 and 0.290; mean = 0.237 ± 0.033 , and uncorrected $p < 0.05$. Significant values across contiguous narrow-band frequencies have been grouped together for ease of interpretation.

† Significant with Bonferroni correction at the level of frequencies.

* Significant after partial correlation correction to age of subjects, via modified τ with uncorrected $p < 0.05$.

Confusion Matrix from Classification Results				
		CI-Predicted Class		
		Normal	Mild/Mod.	Severe
CI-True Class	Normal	26	2	3
	Mild/Mod.	2	3	2
	Severe	1	5	7

Table 4: Resulting confusion matrix from the 5-fold cross-validated, cost-sensitive classification scheme for all $n = 51$ children based on costs in Table 1. Rows represent true class labels, with columns as the predicted labels from the classification.